TESS Asteroseismic Predictions for Red Giants using Machine Learning

M. Schofield[1,2]⋆, G. R. Davies[1,2], W. J. Chaplin[1,2], M. F. Randrianandrasana
[1]Department of Physics and Astronomy, the University of Birmingham, Birmingham B15 2TT, UK
[2]Stellar Astrophysics Centre (SAC), Department of Physics and Astronomy, Aarhus University, Ny Munkegade 120, DK-8000 Aarhus C, Denmark

Last updated 2017 May 31; in original form 2017 May 31

ABSTRACT
Summary: This paper presents a method to predict Red Giant mode detectability with TESS using a Machine Learning Classifier. It requires only the global parameters $\Delta\nu$, $\nu_{\rm max}$, [M/H], $T_{\rm eff}$, the stellar magnitude and length of observation.
Method: Lightcurves for *Kepler* stars with fitted radial mode frequencies were used to generate equivalent TESS lightcurves. The length of observation was reduced, *Kepler* white noise was removed, the bandpass was adjusted, and TESS white noise was added. A detection test was then run on 3 observed modes in these 'TESS-like' lightcurves. Classifiers were then used to predict mode detectability with TESS based upon the global asteroseismic and spectroscopic parameters. The Classifier successfully predicted mode detectability in the original *Kepler* stars, and for 1 year of TESS-like data.
Application: By changing only the length of dataset, instrumental noise level and bandpass of observation, this tool can make solar-like detection predictions for any future mission such as K2, PLATO or CoRoT. It can be make predictions and select targets much faster than traditional detection tests. It is especially useful in an age of extremely large datasets from MAST and Gaia (Eisenstein et al. (2011), Gaia Collaboration et al. (2016)).

1 INTRODUCTION

Satellites such as *Kepler* have allowed asteroseismology of solar-like and Red Giant stars to advance rapidly since the last century Chaplin & Miglio (2013). Power spectra can now be resolved to detect individual modes of oscillation in Main Sequence and Red Giant stars (Lund et al. (2017), Davies & Miglio (2016)).

Future space missions such as TESS (Ricker et al. 2014), K2 (Howell et al. 2014), CoRoT (Baglin et al. 2006) and PLATO (Rauer et al. 2014) will add to our understanding of stellar structure and evolution. These missions will provide a large amount of high-precision data. More than ever, the field of stellar astrophysics will require tools to perform big-data analysis (Kremer et al. 2017).

One of the tools than can be used to handle this larger amount of data is Machine Learning. In this work, Machine Learning was used to create a TESS target selection function using the set of *Kepler* Red Giant stars from Davies & Miglio (2016). This publicly-available algorithm[1] can be downloaded and used as a target selection function for any future space mission.

In most situations Machine Learning is used to solve problems in one of two ways, either using Supervised or Unsupervised Learning. Supervised Learning involves problems where there is a known result.

Supervised Learning has been used to classify types of variable star using previously labelled data (Nun et al. (2014), Elorrieta et al. (2016)). This previously labelled data is known as training data: this is used to train the Machine Learning algorithm. In the problem of variable stars, lightcurves that had already been classified were used to train the algorithm (this is the training dataset). This algorithm was then used to classify the lightcurves of unidentified stars (this is known as the testing dataset).

In Unsupervised Learning, there are no known results (labels). The aim of Machine Learning in this case would be to find trends between variables. This could be used to identify similar stars by analysing their lightcurves without using previously labelled data (for example, Valenzuela & Pichara (2018)).

The aim of this work is to use Machine Learning to make predictions about mode detection probability ($P_{\rm det}$). In this case, $P_{\rm det}$ is a known label, so this is a Supervised Learning problem[2].

Within Supervised Learning, two common algorithms that are used are Classification and Regression. In Regression, the relationship between variables is interpreted using a measure of uncertainty (such as using χ^2 tests). Models are fitted using the independent data, and uncertainty is measured. The models are then improved by reducing this uncertainty. Note that regression is used when the label is continuous. For example, predicting the magnitude of a star is a problem suited to regression, as a star can have any magnitude.

Conversely, Classification algorithms work by assessing similarity[3]. In Classification, the training set is separated into groups based on the similarity of the data. The more information that was gained by splitting the data, the better. For example, if the problem were to separate Red Giant stars from Main-Sequence stars, a star could be classified as either a Red Giant (1), or not a Red Giant

[1] https://github.com/MathewSchofield/TRG

[2] https://machinelearningmastery.com
[3] http://www.simafore.com

(0). In this example, having a Luminosity above $\sim 10L_\odot$ would be a strong indicator that the star was a Red Giant so the data could be separated into groups here. The Classifier would continue to separate the dataset until the Red Giant and Main Sequence samples were distinct. This is not the only problem where Classification can be used on Red Giant stars (Ness et al. (2015), Wu et al. (2017)).

In this work, individual fitted modes from Davies & Miglio (2016) were used to make asteroseismic predictions for TESS with a Supervised Classifier. By separating the targets into those with detected modes and those without, a Classifier was used to select the optimal targets for future observation.

Firstly, Section 2 descirbes how the size of the datasets were increased to improve the predictive ability of the Classifier. Section 3 then describes how the timeseries' of every star were treated before transforming them to power spectra. Section 4 goes on to describe the detection test that was run on the fitted modes. Every mode was grouped into a discrete class depending upon it's detection probability. Each mode was either very likely to be observed (2), quite likely (1), or unlikely (0).

Lastly, Section 5 describes the classification of stars into a group with detected modes, and a group without. This was done by giving a Supervised Classifier asteroseismic and spectroscopic information on every target from APOKASC (Pinsonneault et al. 2014). 70% of the stars were used to train the Classifier; 30% of the sample was kept to test the algorithm. The Classifier was given the mode detection probabilities of the stars in the training set, before making predictions about mode detectability on the testing set.

The Classifier recognised patterns between the variables in the training set, and successfully made predictions about mode detectability with a 0.97?????% precision for the original *Kepler* data. It achieved a precision of 0.92 for 1 year of TESS-like observation, and 0.74 for 27 days of TESS-like observation.

2 INCREASING THE SIZE OF THE DATASETS

Machine Learning performs best when a large dataset is available to train the algorithm upon. In order to increase the size of the dataset from Davies & Miglio (2016) above 1000, the magnitude of each *Kepler* star was perturbed. Each star had it's magnitude perturbed 100 times before the lightcurves were transformed to TESS-like power spectra.

The noise functions of *Kepler* and TESS were used as PDFs to draw magnitudes from. These were used because they provide realistic distributions of the number of stars at different magnitudes that the satellites observed/will observe. Many more fainter stars are observed because the volume of space that contains stars increases as the distance from the satellite increases.

The noise function of *Kepler* is depends on the *Kepler* magnitude of the star, K_p. This noise function is from Chaplin et al. (2011). It is given by

$$\sigma = \frac{10^6}{c} \times \sqrt{c + 9.5 \times 10^5 \left(\frac{14}{K_p}\right)^5}, \quad (1)$$

where

$$c = 1.28 \times 10^{0.4(12-K_p)+7}. \quad (2)$$

Similarly, the noise function of TESS was estimated using the 'calc noise' IDL procedure (from William Chaplin, private communication), which depends on the I_c−band magnitude of the star and the number of pixels in the photometric aperture used when observing the star. This is given by

$$N_{\rm aper} = 10 \times (n + 10), \quad (3)$$

where n is

$$n = 10^{-5.0} \times 10^{0.4\times(20-I_{\rm mag})}. \quad (4)$$

These noise functions were used as the PDFs to draw stellar magnitudes from. 100 magnitudes were drawn for every *Kepler* Red Giant. The lightcurves of this much larger *Kepler* dataset were degraded to look like TESS observations.

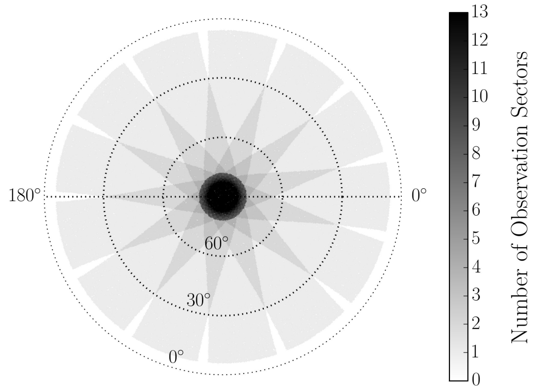

Figure 1. TESS field of view, centred around the ecliptic pole. Each strip will be observed for 27 days before the satellite rotates. Image taken from Campante et al. (2016).

3 TRANSFORMING THE LIGHTCURVES

Before a Classifier could be used on the Red Giants, the timeseries data from *Kepler* needed to be adjusted for a different satellite and mission. This could either be done in the time or frequency domains. Adjustments were made in both domains, and the results were compared.

Several different adjustments needed to be made to the *Kepler* data. One difference between the missions is the length of observation. The *Kepler* mission observed for 4 years, while TESS' nominal 2 year mission will observe stars for between 27 days to 1 year, according to the star's ecliptic latitude (Figure 1). This distinction can be clearly seen when comparing the timeseries', see Figure 2.

As well as reducing the dataset length, the bandpass of observation needed to be adjusted. TESS will observe in a much redder bandpass than that of *Kepler*, Figure 3. This has the effect of reducing the amplitude of stellar signals (i.e the signals due to stellar granulation and oscillation). Campante et al. (2016) found this bandpass correction to be 0.85.

Thirdly, the instrumental noise level in *Kepler* is different to the noise level in TESS. The noise level for the *Kepler* satellite depends on the *Kepler* magnitude of the star, equation 1. This white noise was subtracted from the power spectrum.

As well as subtracting the *Kepler* instrumental noise from the signal, instrumental noise from TESS needed to be added. This noise level was estimated using equation 4, along with the 'calc noise' IDL procedure (from William Chaplin, private communication).

These three adjustments - the length of observation, the bandpass, and the noise level - were performed in both the time and frequency domains for comparison. The methods used are described

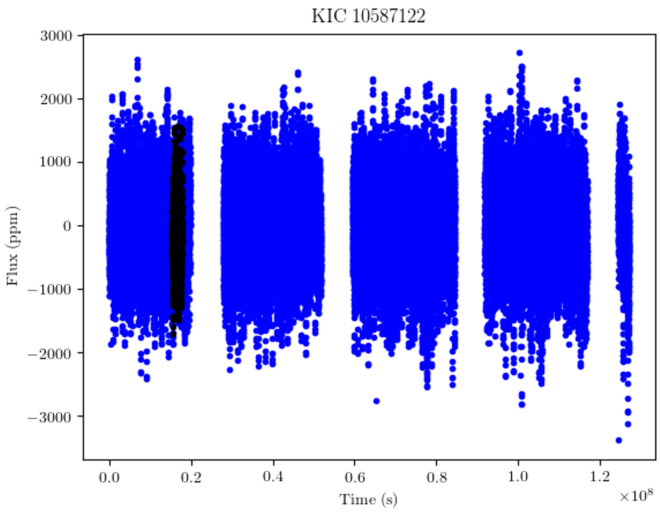

Figure 2. The 4-year long Power Spectra of KIC 10587122 is plotted in blue. Overplotted is the 27-day time segment with most coverage (the period with fewest gaps in the data). Reducing the length of observation this drastically will badly hamper mode detectability.

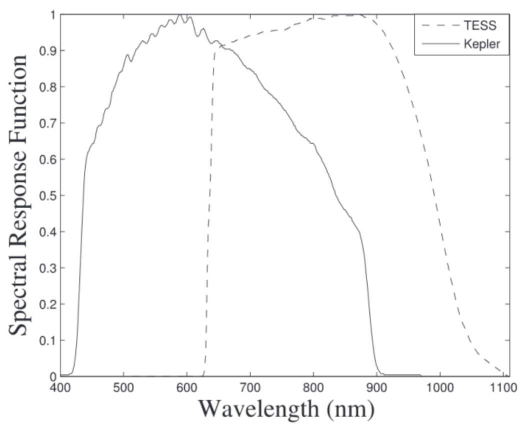

Figure 3. The bandpass of the *Kepler* and TESS missions. TESS will observe at longer (i.e redder) wavelengths than *Kepler*. This will reduce the amplitude of oscillations and granulation, whilst the white noise level will by unaffected. Image taken from Placek et al. (2016).

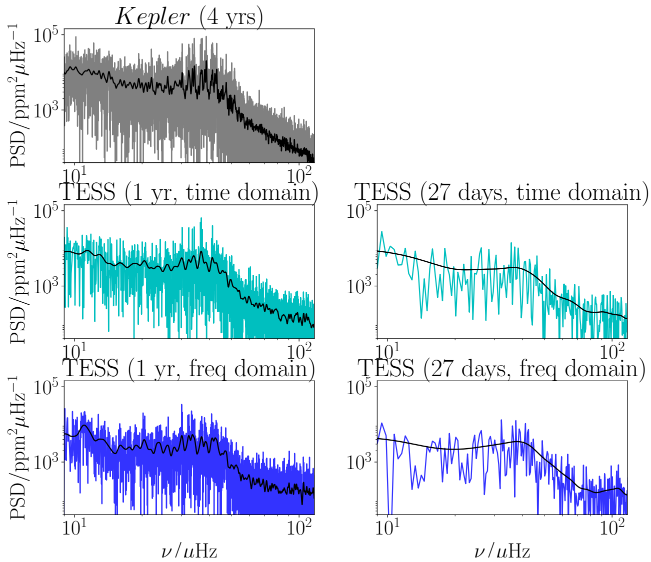

Figure 4. The Power spectra of KIC 10587122 is plotted five times with moving medians in black. The original Power Spectra is plotted in grey. The power spectra after making the data look like TESS are plotted in blue. The data was transformed in the time domain (light blue) or frequency domain (dark blue). The left column shows 1 year of TESS observation (the maximum). The right column shows 27-days (the minimum). Based on this, the time domain was chosen to transform the data in as the background noise level appears lower.

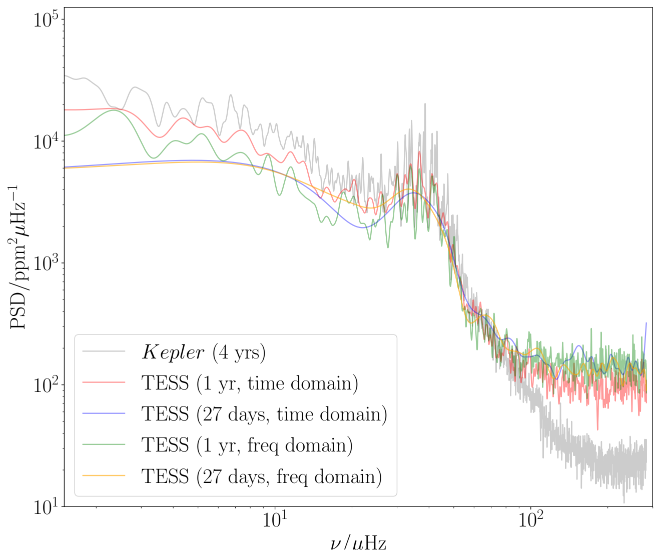

Figure 5. The Power Spectra of KIC 10587122. The original power spectra is in grey. The data was transformed into TESS observation and overplotted. The transformation was done in the time and frequency domains for comparison. Based on this, the time domain was chosen to transform the data in as the background noise level appears lower.

in Figures 6 and 7. The resulting Power Spectra are compared in Figures 4 and 5. After comparing the results, the decision was made to perform adjustments in the time domain before transforming to the frequency domain because the background noise level is lower when the time domain is used to transform .

After adjustments were made in the time domain, power spectra were generated for every star. Power spectra were generated for the original 4-year *Kepler* sample, 1 year of TESS observations and 27 days of TESS observations. A detection test was then run on the radial modes of every star in these 3 datasets.

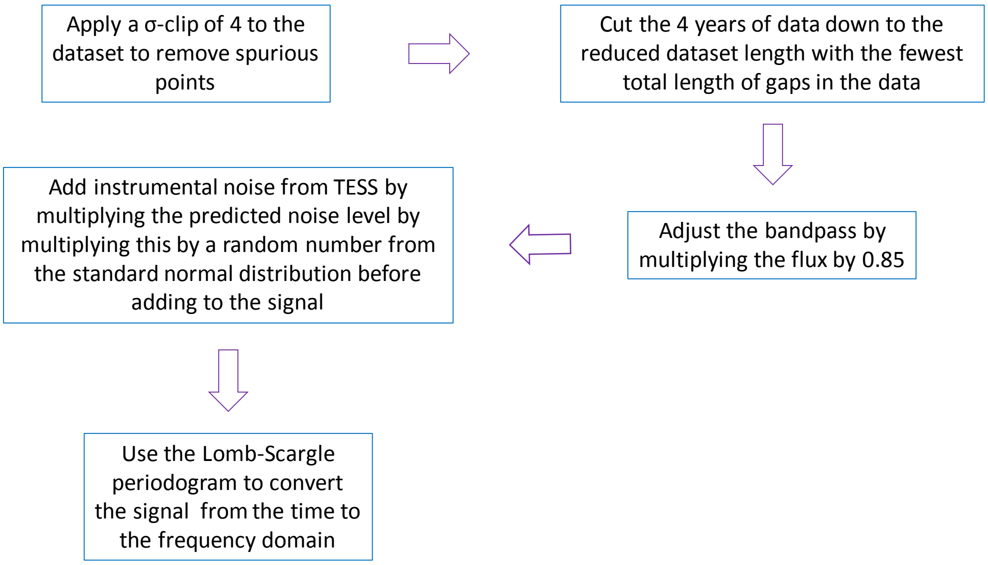

Figure 6. Flow chart of the method to convert the data from *Kepler* to TESS observations in the time domain.

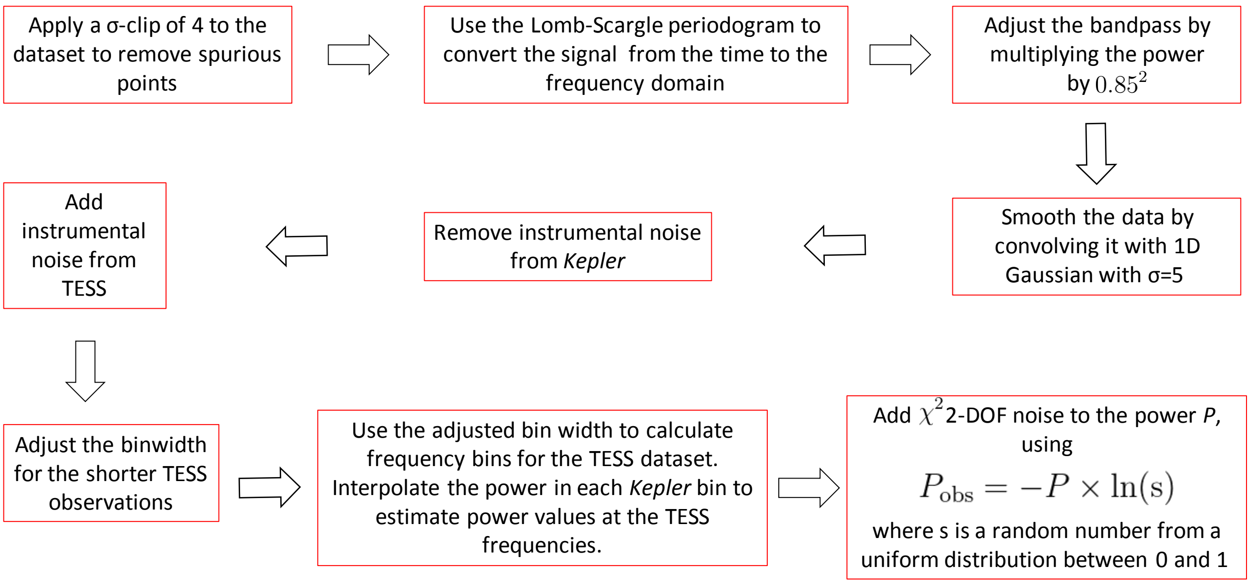

Figure 7. Flow chart of the method to convert the data from *Kepler* to TESS observations in the frequency domain.

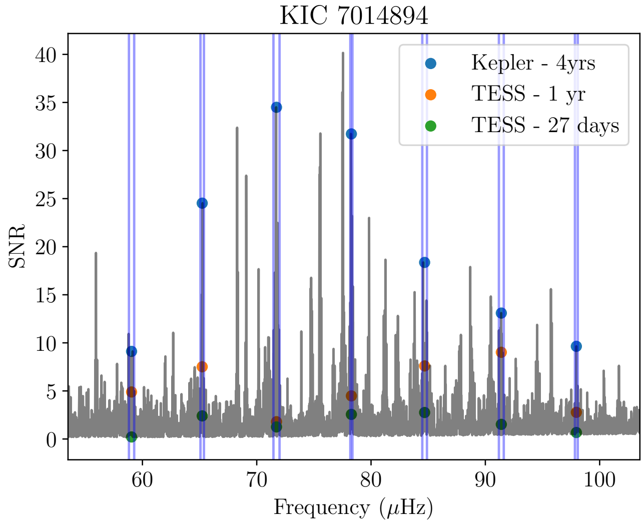

Figure 8. The SNR spectrum of KIC 7014894 after background subtraction. The SNR values of the radial modes in the star were extracted from this spectrum. The values of every mode in the original Kepler spectrum are plotted in blue. The overplotted orange points are the SNR values after degrading the signal to 1 year of TESS observation. Similarly, the green points are the SNR values of 27 days of TESS observations. The white noise level and reduced observation time severely reduce the SNR of

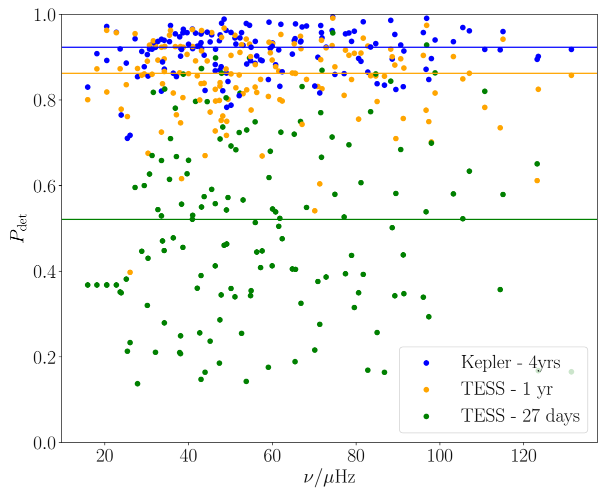

Figure 9. A plot showing the result of the detection test, after running on every mode in 20 stars. The results of the original power spectra are plotted in blue. The results of 1 year of TESS observation are in orange. 27 days of TESS observation is in green. At this short an observation, detecting individual modes will be extremely difficult.

4 DETECTION TEST

Section 3 described the method to transform the *Kepler* lightcurves into TESS-like power spectra. A detection test was then run on the stars to determine which modes were visible after observation by TESS, and which were not.

First, a moving median from Davies & Miglio (2016) was used to estimate the proportion of the signal that was due to white noise and stellar granulation. The solar-like mode envelope width was used as the frequency range of the moving median. This envelope width was calculated as

$$\Gamma_{\rm env} = 0.66 * \nu_{\rm max}^{0.88}, \tag{5}$$

from Mosser et al. (2012). The moving median was used to interpolate between frequencies in the power spectrum. It provided an estimate of the total background in the power spectrum. This background was divided out of the power spectrum to the get Signal-to-Noise spectrum,

$$\mathrm{SNR} = P/B. \tag{6}$$

Once the SNR spectrum for the star was recovered, the SNR values at the mode frequencies were extracted. To ensure the correct SNR values of every mode were used, a window was fitted around each peak-bagged mode frequency. The size of the window was given as the linewidth of the mode. The highest value in the window was taken as the SNR of the mode. An example of this for KIC 7014894 is shown in Figure 8.

Once all mode SNR values for the star were calculated, a detection test was run on each mode (Chaplin et al. 2011), (Campante et al. 2016).

The probability P that the SNR lies above some threshold $\mathrm{SNR}_{\rm thresh}$ is

$$P(\mathrm{SNR} \geqslant \mathrm{SNR}_{\rm thresh}) = p. \tag{7}$$

A false-alarm probability p of 1% was set; there is a 99% chance that the signal is due to solar-like oscillations, rather than noise. Equation 7 is solved for $\mathrm{SNR}_{\rm thresh}$ by substituting P with

$$P = \int_x^\infty \frac{e^{-x}}{\Gamma(N)} x^{N-1} dx. \tag{8}$$

$\Gamma(N)$ is the Gamma function. The lower bound of Equation 8 is set to $x = 1 + \mathrm{SNR}_{\rm thresh}$. N is the number of frequency bins that the mode occupies. The noise in these bins is assumed to follow χ_2 $2n_{\rm bins}$ d.o.f statistics.

Once $\mathrm{SNR}_{\rm thresh}$ is found, Equation 8 is solved again. This time it is solved for P by setting $x = (1 + \mathrm{SNR}_{\rm thresh})/(1 + \mathrm{SNR})$. Here, SNR is the observed Signal-to-noise Ratio calculated from Equation 6. This calculates the probability that the frequency spike was due to stochastic excitation in the convective envelope of the star.

This detection test was applied to every mode of every star in the sample. Figure 9 shows the mode detection probabilities from this test for the original *Kepler* dataset, for 1-year of TESS observation and for 27 days of TESS observation. After these $P_{\rm det}$ values were calculated, a Classifier was used to determine if these results could be predicted rather than calculated. This is described in Section 5.

5 CLASSIFICATION

Section 3 describes how the lightcurves of every star were treated before a detection test was run on the oscillations in Section 4. After this, Classification was applied to the stars to separate them into a suitable target list, and a list of stars that are not suitable for observation with TESS.

It is worth noting that this could be done without using Machine Learning, although it takes much longer. In the age where datasets from missions such as MAST and Gaia (Gaia Collaboration et al. 2016) exist, tools need to be developed to make use of the huge amount of information we now have on stars across the Milky Way. If Machine Learning can replicate the results from a detection test, it could be used as for target selection before future observations. This would reduce the computation time needed to generate a list of targets down by orders of magnitude.

5.1 Preparing the data

Firstly, the detection probabilities of every mode were taken from Section 4. Each probability was changed to a 1 or 0 depending on if a detection was made. For each mode as observed by *Kepler*, the detection threshold was

$$P_{\mathrm{det,Kep}} = \begin{cases} 1 & \text{if } P_{\mathrm{det}} \geqslant 0.9 \quad , \\ 0 & \text{if } P_{\mathrm{det}} < 0.9 \quad . \end{cases} \tag{9}$$

Modes will be more difficult to detect in TESS due to the larger white noise levels and shorter observation times. The threshold for determining a detection was therefore changed;

$$P_{\mathrm{det,TESS}} = \begin{cases} 2 & \text{if } 1.0 \geqslant P_{\mathrm{det}} > 0.9 \quad , \\ 1 & \text{if } 0.9 \geqslant P_{\mathrm{det}} > 0.5 \quad , \\ 0 & \text{if } 0.5 \geqslant P_{\mathrm{det}} > 0.0 \quad . \end{cases} \tag{10}$$

Using equations 9 and 10, every mode was assigned a discrete *class* [0, 1 or 2], depending on how high the probability of detection was for that mode. The same three radial modes (*3 labels*) were used for every star: the mode closest to the centre of the power-excess due to solar-like oscillations $\nu_{\mathrm{max;n}}$, the radial mode one overtone below that $\nu_{\mathrm{n-1}}$, and one overtone above that, $\nu_{\mathrm{n+1}}$ [P_{det} (1), P_{det} (2), P_{det} (3)]. It was important to use the same information for every star so that the algorithm could be trained on the patterns between the variables.

A classifier is an algorithm that can learn a relationship between variables. The classifier will map from some initial information about the star (the X data), to some unknown information (the Y data). In this work, the X data were magnitude (K_p or I_{mag}), ν_{max}, $\Delta\nu$, T_{eff} and [Fe/H]. The Y data labels were P_{det} values for 3 radial modes, centred around ν_{max}.

The more samples available, the better the classifier will be able to learn the relationship between variables. (Davies & Miglio 2016) had peak-bagged 1000 Red Giant stars. In order to increase the number of samples, the stellar magnitude was perturbed 100 times iteratively for every star. The noise level for the star was adjusted in each iteration using equations 1 and 4. A detection probability was calculated for the modes. After removing gaps in the data, this left 60,000 samples to perform Classification upon. An example of the final dataset for 1 year of TESS-like observations are shown in Tables 1 and 2.

5.2 Target selection using a Classifier

The 60,000 samples were separated into a training dataset, and a testing set. 70% of the samples were used to train the classifier (46,410 stars); 30% of the stars were used to test the algorithm (19,890 stars). To train the Classifier, the X and Y data in the training set was given to the algorithm (X_{train} and Y_{train}). Once the Classifier had been trained, the X data from the testing set was given to it (X_{test}). The Classifier then predicted a set of Y data for the testing set (Y_{pred}). This was compared to the actual Y data for the testing set (Y_{test}). The more similar Y_{pred} is to Y_{test}, the better the Classifier replicated the data.

Two metrics were used to measure the performance of the algorithm. The first was the precision of the Classifier, weighted across the classes [0, 1, 2] and the detection probability labels P_{det} (1), P_{det} (2) and P_{det} (3). The second was the Hamming loss[4] of the algorithm. This was used to give a measure of similarity between the two datasets Y_{pred} and Y_{test};

$$H_{\mathrm{loss}}(Y_{\mathrm{test}}, Y_{\mathrm{pred}}) = \frac{1}{n_{\mathrm{labels}}} \sum_{j=0}^{n_{\mathrm{labels}}-1} 1(Y_{\mathrm{pred}} \neq Y_{\mathrm{test}}) \, . \tag{11}$$

Hamming loss score of 0.0 means that Y_{pred} is identical to Y_{test}. A score of 1.0 measn that there are no similar values between Y_{pred} and Y_{test}. The precision and Hamming loss of the Classifier on the *Kepler* and TESS datasets are shown in Table 3.

KIC	Iteration	ν_{max}	$\Delta\nu$	T_{eff}	[M/H]	I_{mag}
9205705	1	25.23	3.181	4685	-0.39	9.89
9205705	2	25.23	3.181	4685	-0.39	9.19
9205705	3	25.23	3.181	4685	-0.39	9.79
9205705	4	25.23	3.181	4685	-0.39	11.30
...						
9205705	100	25.23	3.181	4685	-0.39	7.81
2554924	1	33.97	3.967	4594	0.27	8.46
2554924	2	33.97	3.967	4594	0.27	9.26
...						

Table 1. An example of the X-dataset for 1 year of TESS-like observations. The same star has it's magnitude perturbed 100 times. White noise is then added to the timeseries and mode detection probabilities are calculated for 3 radial modes centred around ν_{max}. Lastly, these probabilities are put into discrete classes [0, 1 or 2]. The radial mode closest to $\nu_{\mathrm{max}}$is labelled P_{det} (2). See Table 2 for the equivalent Y-dataset.

KIC	Iteration	P_{det} (1)	P_{det} (2)	P_{det} (3)
9205705	1	1	2	2
9205705	2	1	2	2
9205705	3	1	2	2
9205705	4	1	2	1
...				
9205705	100	1	2	2
2554924	1	2	2	2
2554924	2	2	2	2
...				

Table 2. An example of the Y-dataset for 1 year of TESS-like observations. These are the mode detection probabilities for 3 radial modes centred around ν_{max}. These probabilities are put into discrete classes [0, 1 or 2]. The radial mode closest to $\nu_{\mathrm{max}}$is labelled P_{det} (2). See Table 1 for the equivalent X-dataset.

Dataset	T_{obs}	Classifier Precision	Hamming loss
Kepler	4 years	0.97?	0.02?
TESS	1 year	0.92	0.07
TESS	27 days	0.74	0.26

Table 3. Results of the Classifier on the original *Kepler* dataset, and the 1-year and 27-day TESS datasets. The 'Classifier Precision' column gives the average weighted precision of the Classifier across the 3 classes [0, 1, 2] and 3 labels [P_{det} (1), P_{det} (2), P_{det} (3)].

[4] http://scikit-learn.org

6 CONCLUSION

For the first time, Machine Learning was applied to TESS target selection. 1000 peak-bagged *Kepler* Red Giant stars from Davies & Miglio (2016) were used to determine whether target selection could be done using a Classifier. The number of samples was increased by perturbing stellar magnitudes 100 times for each star. These perturbed magnitudes were drawn from a PDF of the noise function (equations 1 and 4). After removing stars where global parameters or fitted modes were unavailable, this left 60,000 *Kepler* samples.

Once the number of samples was increased, the timeseries of every sample were degraded to transform them into TESS-like observations. The dataset length was reduced, white noise was added to the signal, and the bandpass of observation was reddened. A moving median was calculated for the power spectra of these Red Giants to estimate the total background in the signal. This was divided out of the spectra, leaving a Signal-to-Noise ratio at every frequency bin (equation 6).

A detection test was run on the SNR values at every mode frequency. This gave a detection probability $P_{\rm det}$ between 0.0 and 1.0 for every mode. In order to prepare the detection probabilities before Classification, each continuous $P_{\rm det}$ value was assigned a discrete class ([0,1 or 2]; equations 9 and 10).

A Classifier was then given the global asteroseismic and spectroscopic properties of the Red Giant sample, along with mode detection probabilities for each star. The parameters [$\nu_{\rm max}$, $\Delta\nu$, $T_{\rm eff}$, [M/H], K_p] from APOKASC (Pinsonneault et al. 2014) were used as the 5 X-data labels. The $P_{\rm det}$ values of 3 radial modes centred around $\nu_{\rm max}$ were used as 3 Y-data labels. The classifier successfully used the global stellar parameters (the X-data) to make predictions about mode detectability (the Y-data). The stars with the largest number of detected modes could then be selected as the Red Giants for observation by TESS.

The Classifier successfully made predictions about the original 4 years of Kepler data; the algorithm had a weighted precision 0.97????????????? across the 3 $P_{\rm det}$ labels. This confirms the proof of concept that Classifiers can be used as a way to select targets before future missions. Classification vastly reduces the computation time required to produce a target selection function, especially when large datasets are involved ($\geqslant 50,000$ stars).

Degrading the Red Giant data to make predictions for 1 year of TESS observations was also successful. The predicted mode detections scored a weighted precision of 0.92 across the 3 $P_{\rm det}$ labels. This illustrates that Classification is a valid target selection method for TESS targets in the Continuous Viewing Zone (CVZ, (Ricker et al. 2014)). Using the Classifier on 27 days of TESS data returned detection predictions with a precision of 0.74. This is because for 27 days of TESS observations, the white noise level is too high and the length of observation is too short to make robust predictions of individual solar-like oscillations.

REFERENCES

Baglin A., et al., 2006. p. 3749, http://adsabs.harvard.edu/abs/2006cosp...36.3749B

Campante T. L., et al., 2016, preprint, 1608, arXiv:1608.01138

Chaplin W. J., Miglio A., 2013, Annual Review of Astronomy and Astrophysics, 51, 353

Chaplin W. J., et al., 2011, The Astrophysical Journal, 732, 54

Davies G. R., Miglio A., 2016, arXiv:1601.02802 [astro-ph]

Eisenstein D. J., et al., 2011, The Astronomical Journal, 142, 72

Elorrieta F., et al., 2016, Astronomy and Astrophysics, 595, A82

Gaia Collaboration et al., 2016, Astronomy and Astrophysics, 595, A2

Howell S. B., et al., 2014, Publications of the Astronomical Society of the Pacific, 126, 398

Kremer J., Stensbo-Smidt K., Gieseke F., Steenstrup Pedersen K., Igel C., 2017, preprint, 1704, arXiv:1704.04650

Lund M. N., et al., 2017, The Astrophysical Journal, 835, 172

Mosser B., et al., 2012, A&A, 537, A30

Ness M., Hogg D. W., Rix H.-W., Ho A. Y. Q., Zasowski G., 2015, The Astrophysical Journal, 808, 16

Nun I., Pichara K., Protopapas P., Kim D.-W., 2014, The Astrophysical Journal, 793, 23

Pinsonneault M. H., et al., 2014, The Astrophysical Journal Supplement Series, 215, 19

Placek B., Knuth K. H., Angerhausen D., 2016, Publications of the Astronomical Society of the Pacific, 128, 074503

Rauer H., et al., 2014, Experimental Astronomy, 38, 249

Ricker G. R., et al., 2014, Journal of Astronomical Telescopes, Instruments, and Systems, 1, 014003

Valenzuela L., Pichara K., 2018, Monthly Notices of the Royal Astronomical Society, 474, 3259

Wu Y., et al., 2017, preprint, 1712, arXiv:1712.09779

This paper has been typeset from a TEX/LATEX file prepared by the author.